

special communication

Focal extracellular potential: a means to monitor electrical activity in single cardiac myocytes

TARA L. RIEMER AND LESLIE TUNG

Department of Biomedical Engineering, Johns Hopkins University, Baltimore, Maryland 21205

Riemer, Tara L., and Leslie Tung. Focal extracellular potential: a means to monitor electrical activity in single cardiac myocytes. *Am J Physiol Heart Circ Physiol* 278: H1383–H1394, 2000.—The focal extracellular potential (FEP) described in this study is an electrophysiological signal related to the transmembrane potential (V_m) of cardiac myocytes that avoids the mechanical fragility, interference with contraction, and intracellular contact associated with conventional whole cell recording. One end of a frog ventricular myocyte was secured into a glass holding pipette. The FEP was measured differentially between this pipette and a bath pipette while the cell was voltage- or current-clamped by a third whole cell pipette. The FEP appeared as an amplitude-truncated action potential, while FEP duration accurately reflected the action potential duration (APD) at 90% repolarization (APD₉₀). FEP magnitude increased as the holding pipette K^+ concentration ($[K^+]$) was increased. The FEP-voltage relation was quasi-linear at negative V_m with a slope that increased with elevated holding pipette $[K^+]$. Increasing the membrane conductance inside the holding pipette by adding amphotericin B or cromakalim linearized the FEP-voltage relation across all V_m . The FEP accurately reported electrical activation and APD₉₀ during changes of stimulation frequency and episodes of cellular stretch.

action potential duration; cardiac electrophysiology; voltage clamp; frog

BECAUSE THE HEART is inherently both a mechanical and an electrical organ, techniques for measuring electrical activity that minimize the interference with mechanical signals and events are especially valuable. The electrocardiogram (ECG), for example, is derived from the electrical fields and currents representing the mass electrical activity of a large population of cells. It is therefore large enough to be recorded transthoracically without mechanically impacting the heart in any way. Conversely, the electrical signals from isolated cardiac cells are too small to be measured at any practical distance from the cell. Modern recording techniques,

such as tight-seal microelectrode patch recording, whole cell recording, and microelectrode impalement, have submillivolt resolution but require direct access to the interior of the cell. These techniques are generally satisfactory for purely electrical recordings, but maintaining this electrical access to the intracellular space while attempting to measure or control mechanical parameters such as force or cell length is difficult.

Simultaneous recordings of mechanical and electrical parameters are necessary to study cardiac excitation-contraction (EC) coupling (the conversion of an electrical action potential to cellular contraction) and mechano-electrical (ME) coupling (the impact of mechanical events on the electrical state of the heart) (11, 18). To measure cellular force or apply a controlled mechanical stretch during EC or ME coupling studies, one must anchor the cell at both ends in addition to monitoring the cell electrically. Only a few EC coupling studies (35, 37, 40) and ME coupling studies (32, 41) of this type exist for single cardiac myocytes, mainly because of the difficulty of the available techniques for attaching and stretching a single cell (4, 13) and the additional complication introduced to obtain and maintain simultaneous electrical recordings using traditional electrophysiological techniques. Indeed, we have attempted to use conventional whole cell electrical recordings while stretching cells (27, 39) but have achieved very limited success because of the extreme experimental challenges.

Some important electrophysiological questions regarding single cardiac cells can be explored solely by measuring action potential duration (APD) without voltage measurements as precise as those achieved from traditional microelectrode techniques. For example, APD has been of central importance in studies on pharmacological effects (19, 26) and stimulation rate (36), as well as in EC coupling experiments exploring the effects of heart failure (21), cardiac hypertrophy (5), and myocardial infarction (20). In the ME coupling literature, the question of whether APD shortens or lengthens in response to cell or tissue stretch remains disputed (11).

APD is also clinically relevant. Long Q-T syndrome, caused by delayed repolarization and a prolonged APD,

The costs of publication of this article were defrayed in part by the payment of page charges. The article must therefore be hereby marked "advertisement" in accordance with 18 U.S.C. Section 1734 solely to indicate this fact.

is associated with torsades de pointes, a polymorphic ventricular tachycardia (1). In addition, cells in different regions of the heart (epicardial, midmyocardial, and endocardial layers) are characterized by their different APDs (42), resulting in varying repolarization times throughout the heart wall. Such dispersion of repolarization has been hypothesized as a substrate for reentrant activity (16) and may contribute to the development of torsades de pointes (2). In addition, early repolarization leading to a shortened APD is often observed during episodes of cardiac ischemia (3, 9).

Because of the unequivocal importance of the APD, a less invasive method for measuring the action potential duration and timing without the technical difficulties of traditional microelectrode or patch pipette techniques would become highly advantageous. One such method, using voltage-sensitive fluorescent dyes, has been used to measure relative transmembrane potential (V_m) changes in single cells (7). However, this technique is highly sensitive to motion of the recording site, and the dyes can become toxic with prolonged exposure to light (33).

Our approach was motivated by the sucrose gap (23) and monophasic action potential (MAP) (12) methods for electrophysiological recording from cardiac tissue or whole heart preparations. In each case, the recorded potential is a fraction of the true V_m that develops from a region of partially isolated and depolarized tissue. This study determines the feasibility and limits for recording analogous potentials from isolated and depolarized portions of single cells.

In our new technique, a large extracellular pipette is affixed to the end of a cell to monitor V_m . The region of cell membrane inside the pipette is depolarized locally using an elevated KCl solution resulting in a decreased access resistance to the intracellular space. Recordings from this pipette indicate whether the cell is excited as well as the timing of the beginning and end of the action potential. The method is also mechanically stable. The recording pipette can be used to secure the cell during axial stretches to measure or determine cell length or force while monitoring the electrical state of the cell.

Preliminary versions of this study have been presented in abstract form (29, 30).

METHODS

Cell Preparation

Single ventricular cells were obtained by enzymatic dissociation of the whole frog heart (*Rana pipiens*) by Langendorff retrograde perfusion as previously described (38). The enzyme solution consisted of 309 U/ml collagenase type II (Worthington Biochemical, Lakewood, NJ) and 6,450 U/ml trypsin (bovine pancreas, Sigma Chemical, St. Louis, MO) in normal extracellular Ringer solution. After the isolation procedure, the heart was stored at 6°C in low calcium Ringer solution. All experiments were conducted at room temperature (22–25°C) in normal extracellular Ringer solution.

Solutions

Normal extracellular Ringer solution contained (in mM) 110 NaCl, 3 KCl, 1 CaCl₂, 10 HEPES, and 10 glucose (pH 7.25). Low calcium Ringer solution contained 0.2 mM CaCl₂

Table 1. *Holding pipette solution components*

| K ⁺ Solution | NaCl, mM | KCl, mM | K-Glutamate, mM | CaCl ₂ , mM | HEPES, mM |
|-------------------------|----------|---------|-----------------|------------------------|-----------|
| 3 mM | 110 | 3 | 0 | 0.1 | 10 |
| 20 mM | 100 | 20 | 0 | 0.1 | 10 |
| 40 mM | 80 | 40 | 0 | 0.1 | 10 |
| 70 mM | 50 | 30 | 40 | 0.1 | 10 |
| 100 mM | 20 | 30 | 70 | 0.1 | 10 |

and was otherwise identical to normal extracellular Ringer. The standard internal pipette solution for conventional whole cell clamp experiments contained (in mM) 10 NaCl, 30 KCl, 70 K-glutamate, 5 EGTA, 10 HEPES, and 5 MgATP (pH 7.20). Low ATP pipette solution contained 1 mM MgATP and was otherwise identical to the standard internal pipette solution. Holding pipette solution components varied as detailed in Table 1.

Cromakalim (Sigma), an ATP-sensitive K⁺ channel (K_{ATP}) agonist, was included in the holding pipette for selected cells at a concentration of 100 μmol/l. Amphotericin B (Sigma), a membrane pore-forming antibiotic used in the perforated patch method (25), was included in the holding pipette solution during some experiments. When amphotericin B was used, the tip of the holding pipette was first dipped into antibiotic-free extracellular solution, and then the pipette was back-filled with extracellular solution containing 240 μg/ml amphotericin B (25).

Focal Extracellular Potential Recordings

Two glass holding pipettes each with a tip diameter of ~2–4 μm were mounted on motorized three-dimensional manipulators. One holding pipette ("reference") was filled with extracellular Ringer solution; the other pipette ("active") was filled with holding pipette solution (Table 1). Ag-AgCl electrodes inserted into the back of each pipette were connected to the differential inputs of a DC amplifier (Grass P16 Micro Electrode DC Amplifier, Grass Instruments, Quincy, MA). The amplifier ground was connected to the bath solution and the ground of the patch clamp unit. The focal extracellular potential (FEP) is defined as the voltage difference between the reference and active holding pipettes (Fig. 1A).

Both holding pipettes were lowered into a chamber containing cells dispersed in extracellular Ringer solution. Suction was used to draw the end of a single cell into the lumen of the active pipette (Fig. 1B). The reference pipette approached or held the opposite end of the cell. At least 2 min elapsed after this configuration was achieved before FEP recording commenced. Any DC offset in the FEP signal was either zeroed manually before recording or subtracted digitally following data acquisition.

Whole Cell Clamp Recordings

For validation studies of the FEP, an additional patch pipette was attached to the cell for current- or voltage-clamp recordings. Conventional whole cell clamp recording techniques (15) were implemented using glass pipettes with a tip diameter of ~1 μm and a resistance of 2–5 MΩ. Triggered action potentials were generated under current clamp conditions by a 5-ms depolarizing current pulse using a commercial patch clamp unit with a grounded bath electrode (PC-One Patch Clamp, Dagan, Minneapolis, MN). When the current or voltage clamp is used to verify the FEP signal, the patch clamp unit was required to be of the type using a grounded bath, because we observed that a driven bath causes large capacitive artifacts that obscure the true FEP signal.

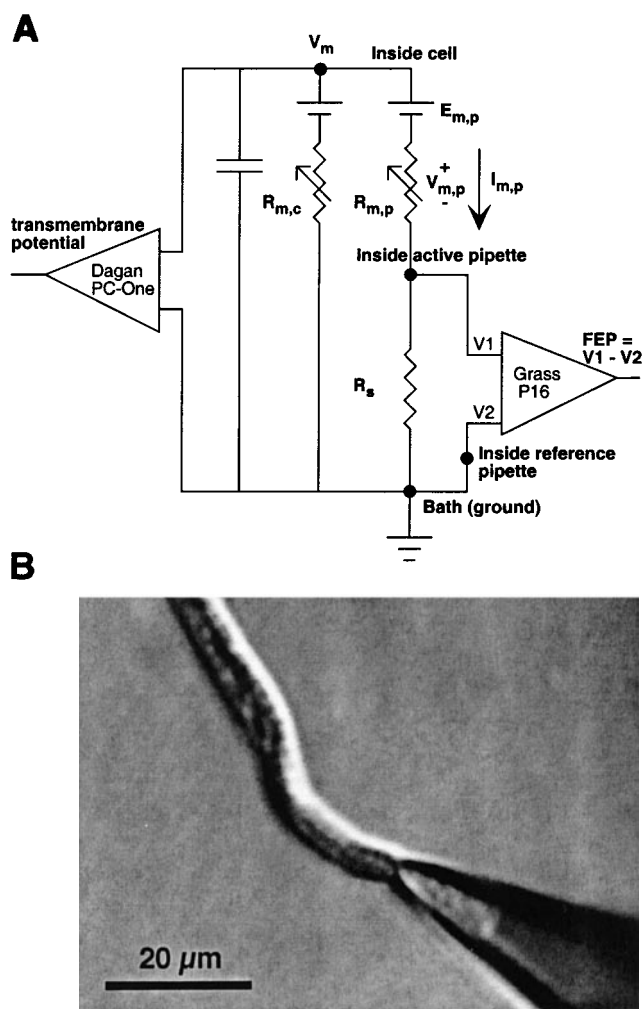


Fig. 1. Experimental recording configuration. *A*: simplified equivalent circuit for cell in focal extracellular potential (FEP) and whole cell clamp recording configuration. V_m , transmembrane potential of cell; $I_{m,p}$, current through membrane patch inside holding pipette; $E_{m,p}$, driving potential of this membrane patch; $V_{m,p}$, potential drop across this membrane patch; $R_{m,p}$, resistance of this membrane patch; $R_{m,c}$, resistance of membrane of remainder of cell; R_s , seal resistance of holding pipette. *B*: light micrograph showing a frog ventricular cell end inside tip of active holding pipette and $\sim 20\%$ of cell length.

Action potential-shaped, voltage-clamp pulses of eight different durations (137 to 1,094 ms) were based on an action potential with a duration of ~ 550 ms that was recorded at 1 kHz under standard conditions. Action potential clamps of varying durations were generated from this action potential by interpolating time points so that the action potentials were scaled to 25, 50, 75, 100, 125, 150, 175, and 200% of the original duration.

Mounting and Stretching an Individual Myocyte

To measure the FEP during cell stretch, we grasped a frog ventricular cell at both ends using the active and reference holding pipettes. The cell was then mounted around a 50- μm glass optical fiber. The glass probe was displaced under fine piezoelectric control to precisely control cell length and measure cell force, as previously described (39). Cells were paced by field stimulation at 0.5 Hz while the FEP and force

were continuously recorded. The whole cell patch pipette was not used during these experiments.

Computer Simulations

Isochronal current-voltage relations were simulated by implementing a biophysical model for the frog ventricle (28) using MATLAB software (MathWorks, Natick, MA). Standard conditions were used unless otherwise specified. Current-voltage relations were simulated using a 1,000-ms voltage clamp to the test potential from a resting potential of -85 mV.

Data Collection and Analysis

All recordings were captured using a data acquisition board (Lab-NB, National Instruments, Austin, TX) in a desktop computer (Macintosh 7100 Power PC, Apple Computer, Cupertino, CA) running customized software (LabVIEW, National Instruments). Up to four channels of data were acquired simultaneously at a sampling rate of 1 kHz per channel.

APD was measured at 90% repolarization (APD_{90}) and was calculated by determining the time elapsed from the action potential upstroke to the point of 90% repolarization from the maximum overshoot. The upstroke time was defined as the instant of maximum rate of rise in V_m . FEP signals were digitally filtered with a second-order low-pass digital Butterworth filter with a cutoff frequency of 50 Hz using MATLAB software. Duration of the FEP signal was measured as the time elapsed between the maximum rate of rise and the maximum rate of fall of the filtered signal.

RESULTS

FEP Response to Triggered Action Potentials

Before the active holding pipette grasped the cell, the whole cell pipette was tightly sealed to the cell, and an action potential was triggered (Fig. 2*A*). Under these conditions, no FEP signal was observed. After the active pipette containing 20 mM K^+ solution (Table 1) grasped one end of the myocyte, a distinct FEP signal in response to triggered action potentials appeared within 2 min (Fig. 2*B*). Upon release of the myocyte by the active pipette, the FEP signal immediately disappeared (Fig. 2*C*). In each case, an identical 5-ms current injection pulse triggered the action potential.

While the holding pipette grasped the myocyte (Fig. 2*B*), the duration of the action potential (APD_{90}) was 542 ms, and the duration of the FEP was 548 ms. The timing of the upstroke of the action potential and FEP differed by only 1 ms, and the timing of the repolarization of the action potential and FEP differed by 5 ms. Although the timing and duration of the FEP closely tracked that of the action potential, the shape of the FEP did not exactly follow the shape of the action potential. Instead, the FEP appears to be an attenuated action potential that has been truncated in amplitude.

Conditions for FEP

Reversibility of FEP. In several cells ($n = 6$ cells), the reversibility of the FEP signal was explored by attaching and releasing the active holding pipette from the cell several times while the FEP and V_m were monitored, as in Fig. 2. In each case, the FEP signal appeared if and only if the myocyte end was inside the

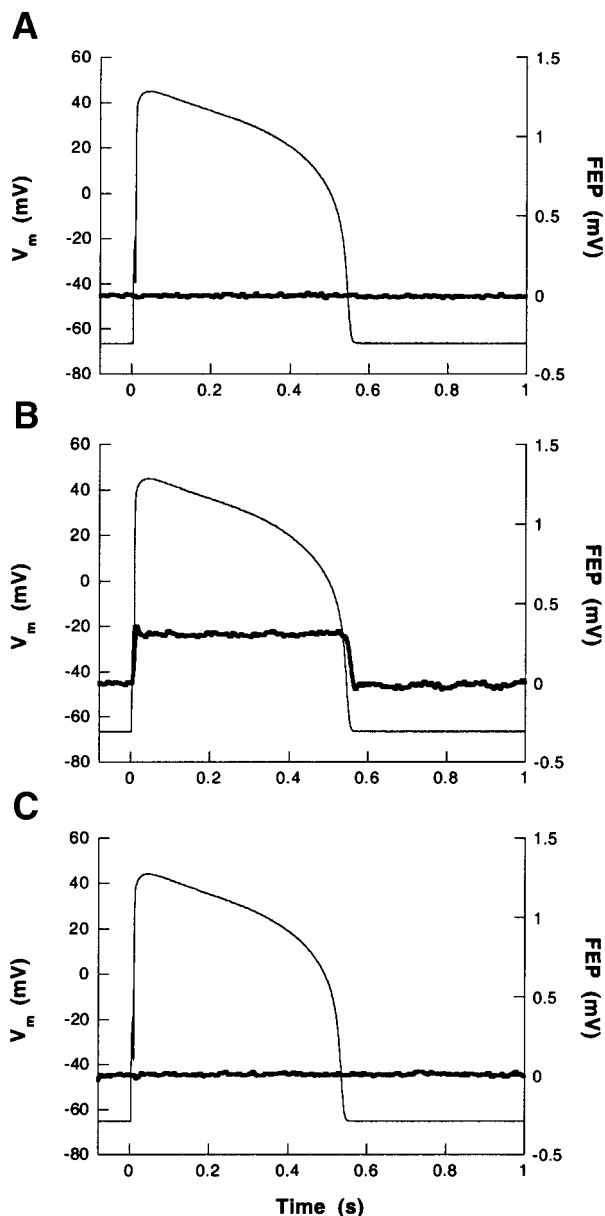


Fig. 2. Action potentials were triggered by current injection. Both V_m during current clamp (light trace) and FEP signal (bold trace) were measured simultaneously. *A*: active holding pipette near cell in bath. *B*: active pipette containing a K^+ concentration ($[K^+]$) of 20 mM grasping one end of cell. *C*: following release of cell end by active pipette.

holding pipette. Pulling a larger amount of the myocyte end into the holding pipette increased the magnitude of the FEP to an extent approximately proportional to the amount of cell inside the holding pipette.

Minimal conditions. Further experiments were conducted with various configurations of the whole cell pipette and electrical stimulus to explore the conditions necessary to record an FEP signal. The presence of the whole cell pipette was not necessary for recording an FEP. Action potentials triggered by both field stimulation and current injection produced similar FEPs. However, the field stimulus coincided with a large transient artifact on the FEP signal that obscured the

action potential upstroke, although the action potential repolarization was still clearly visible. In all cases, the shape of the FEP appeared to be truncated in amplitude compared with the action potential. A subthreshold field stimulus produced only the stimulus artifact on the FEP recording.

Measuring APD

The duration of the FEP signal seems to reflect the duration of the action potential as measured by V_m (Fig. 2*B*). To further define the relationship between these two measures of APD, we applied voltage clamps of various durations to cells. For each cell ($n = 8$), the FEP was recorded while V_m was clamped with eight action potential clamps and seven rectangular voltage clamps (Fig. 3).

For the action potential clamps (Fig. 3*A*), the duration of the action potential (APD₉₀) and of the FEP signal were calculated as described in METHODS. Compiled results showing the average and standard deviation of FEP duration measured for all cells are shown in Fig. 4. The holding pipette contained a K^+ concentration ($[K^+]$) of either 20, 40, or 70 mM for these cells, and no difference in accuracy of the APD measurements was detected for the different levels of $[K^+]$. The duration of the action potential as measured by the FEP recording was between 98.5% and 103.6% of the measured APD₉₀ for all data points.

For all rectangular voltage-clamp recordings (Fig. 3*B*), the duration of the clamp as measured by the FEP recording was within 1% of the actual clamp duration for all recordings from the eight cells.

Dependence on $[K^+]$

Experiments were conducted using holding pipette solutions containing $[K^+]$ ranging from 3 to 100 mM (Table 1). To standardize results from different cells, we used an action potential-shaped voltage-clamp pulse of fixed duration (Fig. 5*A*). Figure 5*B* shows the FEP obtained from cells during the action potential clamps for holding pipettes containing $[K^+]$ of 3, 20, 40, and 70 mM. FEP signals recorded using a holding pipette containing a $[K^+]$ of 100 mM were similar to those for 70 mM.

Although the magnitude of the FEP signal varied from cell to cell, in general, larger holding pipette K^+ concentrations resulted in a larger FEP signal and an improved signal-to-noise ratio. However, cells that were grasped by holding pipettes containing a $[K^+]$ of 70 or 100 mM tended to become significantly depolarized unless they were voltage-clamped to a normal resting potential.

Dependence on V_m

The FEP signal appears to be an amplitude-truncated version of the cellular V_m . The application of successive trapezoidal voltage clamps to a cell shows that the FEP saturates at V_m between -30 and -20 mV (Fig. 6). This point of saturation, or truncation, of the

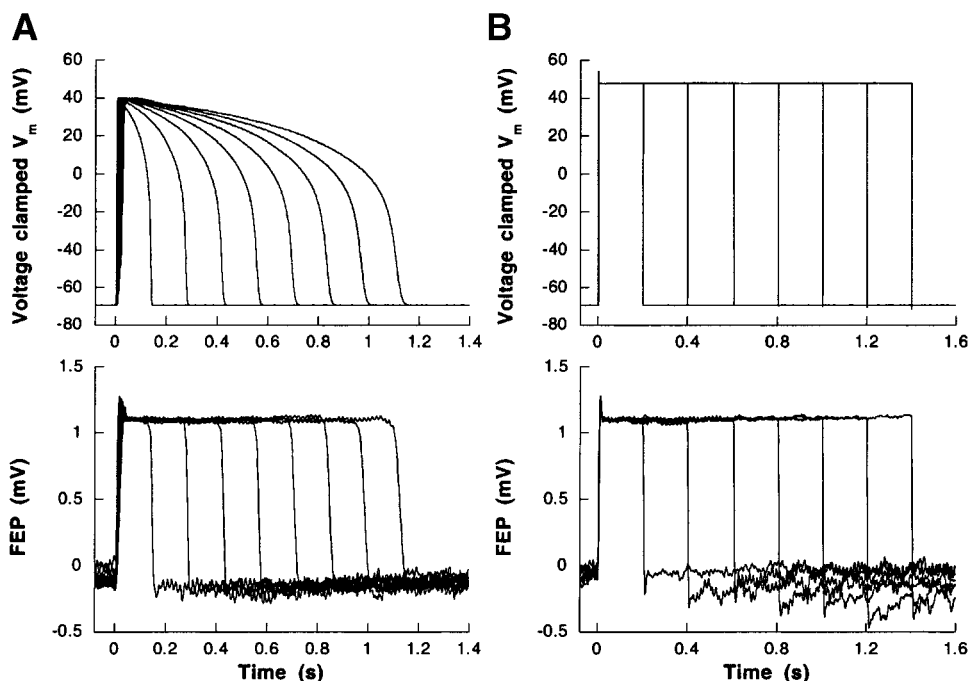


Fig. 3. FEP response to voltage clamps of various durations. *A*: action potential clamps. *Top*, clamped V_m . *Bottom*, FEP responses to action potential clamps. *B*: rectangular voltage clamps. *Top*, clamped V_m . *Bottom*, FEP responses to rectangular voltage clamps. Holding pipette $[K^+]$ was 20 mM during all clamps.

FEP occurs at the same voltage level for each clamp pulse, regardless of the time course of the pulse.

The relationship among V_m , cellular currents, and the FEP was further quantified by applying rectangular voltage clamps of increasing amplitude to myocytes during FEP recording ($n = 20$). V_m was initially held at rest, clamped to a test potential for 1,000 ms, and then returned to rest. For each test pulse, the FEP values between 900 ms and 1,000 ms after the onset of the test potential were sampled and averaged. This average was then corrected for small voltage offsets by subtracting the signal average of the first 100 ms after the return to rest. Isochronal current-voltage relations

were produced by plotting current against pulse voltage. Isochronal FEP-voltage relations were produced by plotting the FEP signal during the test pulse against the pulse voltage.

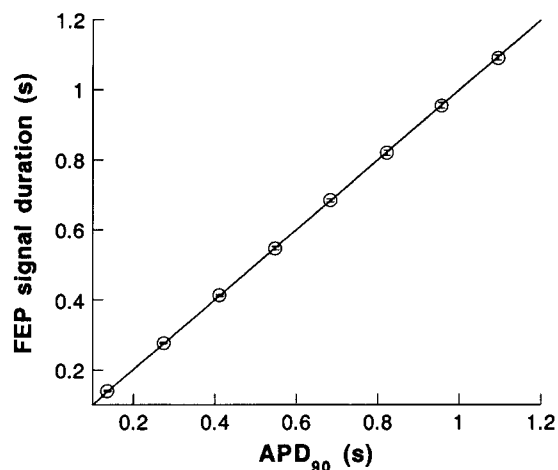


Fig. 4. Comparison of action potential duration (APD) as measured from V_m and FEP recordings. Duration of FEP signal is plotted vs. APD at 90% repolarization (APD_{90}) of applied action potential for 8 cells. Open circles, average FEP duration for all 8 cells; error bars, standard deviation at each APD_{90} . Holding pipette $[K^+]$ was either 20, 40, or 70 mM in these cells. Solid line represents FEP duration equal to APD_{90} .

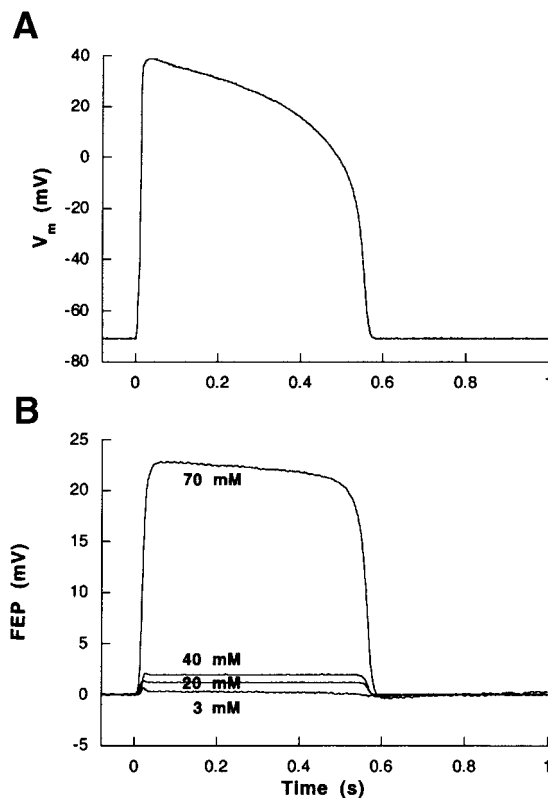


Fig. 5. FEP response to an action potential clamp. Action potential clamp pulse (*A*) and FEP response (*B*) with holding pipette $[K^+]$ of 3, 20, 40, and 70 mM.

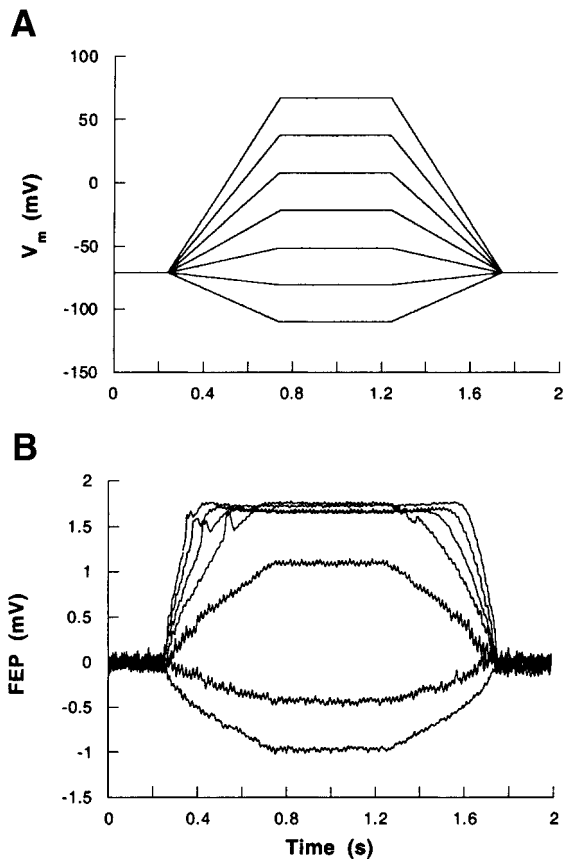


Fig. 6. FEP response to a trapezoidal voltage clamp. Voltage-clamp pulses (A) and FEP responses (B) with a holding pipette $[K^+]$ of 20 mM.

Representative isochronal FEP-voltage relations are shown together with the current-voltage relations for cells with holding pipettes containing $[K^+] = 3, 20,$ or 70 mM (Fig. 7). In each case, the FEP has a nearly linear relationship with a positive slope over a range of negative V_m . This slope increases as the holding pipette $[K^+]$ increases (note the different plot scales for the FEP signal, right ordinate, in Fig. 7A–C). The slopes of the FEP-voltage relations change for values of V_m that are more positive to this linear region. The point of maximum curvature of the FEP-voltage relation, which marks the transition between these two regions of different slope, moves to more positive V_m as $[K^+]$ increases. This transition point is at approximately -60 mV for $[K^+] = 3$ mM (Fig. 7A), -35 mV for $[K^+] = 20$ mM (Fig. 7B), and -15 mV for $[K^+] = 70$ mM (Fig. 7C).

The FEP-voltage relationship mirrors the whole cell current-voltage relation expected for various levels of extracellular K^+ . Figure 8 compares FEP-voltage relations from Fig. 7, plotted on the same scale (Fig. 8A), with simulated current-voltage relations for a frog ventricular cell immersed in an extracellular $[K^+]$ of 3, 20, and 70 mM (Fig. 8B). In both cases, the slope of the FEP-voltage relation at negative transmembrane potentials increases as $[K^+]$ increases. Also, the positive limit of the linear region moves toward more positive V_m with increased $[K^+]$. We hypothesized that the FEP is

related to the currents or conductances of the membrane patch inside the holding pipette.

Increasing Magnitude and Linearity of FEP

Because the FEP appears to be related to the conductance of the membrane tip inside the holding pipette, we hypothesized that the FEP-voltage relation could be linearized by linearizing the current-voltage relation of the membrane tip. We also theorized that the amplitude of the FEP could be increased by increasing the overall conductance of this membrane. Two modifications of the FEP solutions were used to test these

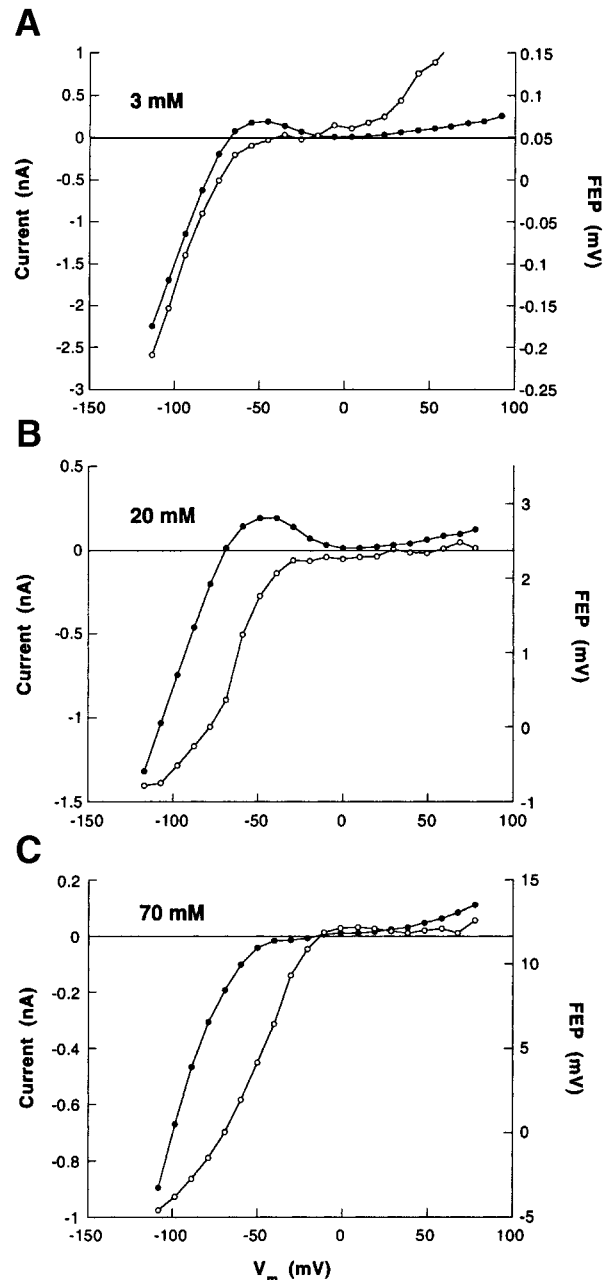


Fig. 7. Relationship between FEP, whole cell current, and V_m . Current-voltage (closed circles) and FEP-voltage relations (open circles) using holding pipette solutions containing $[K^+]$ of 3 (A), 20 (B), and 70 (C) mM. Plot scales for FEP (right ordinate) vary for A–C.

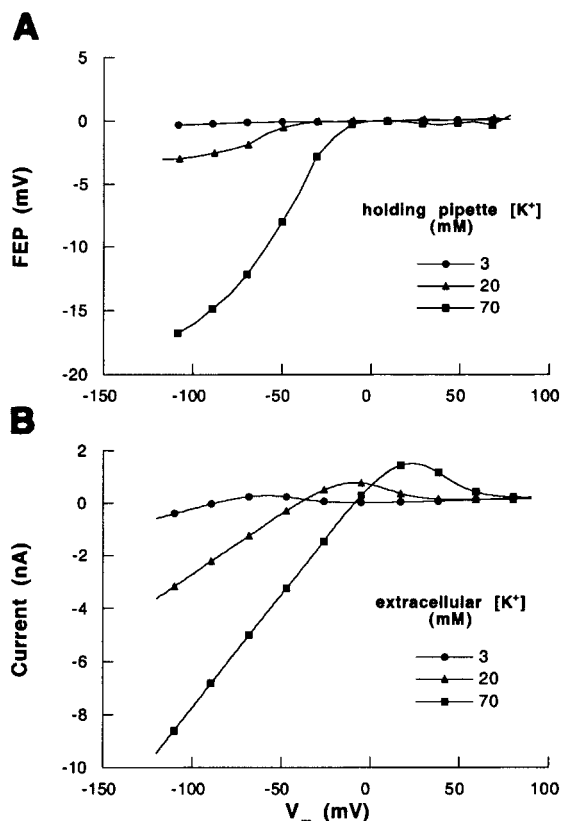


Fig. 8. Comparison of effects of holding pipette and extracellular $[K^+]$. *A*: composite plot of FEP-voltage relations from Fig. 7. *B*: model-simulated current-voltage relations for a frog ventricular cell with extracellular $[K^+]$ of 3, 20, and 70 mM.

hypotheses. First, a large, voltage-insensitive membrane conductance was created by including amphotericin B, an antibiotic that forms membrane pores selectively permeable to small cations (22), in the active holding pipette ($n = 10$). Second, a large outward

conductance was produced by including cromakalim, a K_{ATP} channel agonist, in the holding pipette ($n = 5$).

Amphotericin B. Cells were grasped by active holding pipettes containing 240 $\mu\text{g/ml}$ amphotericin B in normal extracellular solution ($[K^+]$ of 3 mM). As soon as stable FEP and whole cell clamp recordings were achieved, rectangular voltage clamps of increasing amplitude were applied ($n = 4$). FEP-voltage relations were determined as described above, normalized, and plotted in Fig. 9*A* together with normalized relations for holding pipette $[K^+]$ of 20 and 40 mM without amphotericin B. Figure 9*A* shows that with amphotericin B in the active holding pipette, the FEP does not saturate at positive V_m , and the FEP-voltage relation is significantly more linear. The action potential clamp protocol of Fig. 3*A* was repeated with amphotericin B (Fig. 9, *B* and *C*), illustrating that the truncation of the FEP recording with respect to V_m is no longer present. In addition, the FEPs are of a much larger amplitude than those recorded with normal holding pipette solution (containing 3–40 mM K^+ and no amphotericin B) in the active pipette (Figs. 3*A* and 5*B*).

Cromakalim. Frog ventricular cells contain an ATP-sensitive K^+ current ($I_{K,ATP}$) that is sensitive to extracellular application of the K_{ATP} channel agonist cromakalim under conditions of low intracellular ATP (J. S. Fan and L. Tung, unpublished observations). To selectively activate these channels, we used low-ATP internal pipette solution, and cells were grasped by active holding pipettes containing 100 $\mu\text{mol/l}$ cromakalim in 40 mM K^+ holding pipette solution ($n = 4$). The protocols described above for amphotericin B were repeated with cromakalim. Figure 10 shows that the activation of $I_{K,ATP}$ adds an outward current at positive V_m , and this additional current tends to linearize the FEP-voltage relation. In addition, the FEP is a more accurate rendition of the action potential compared

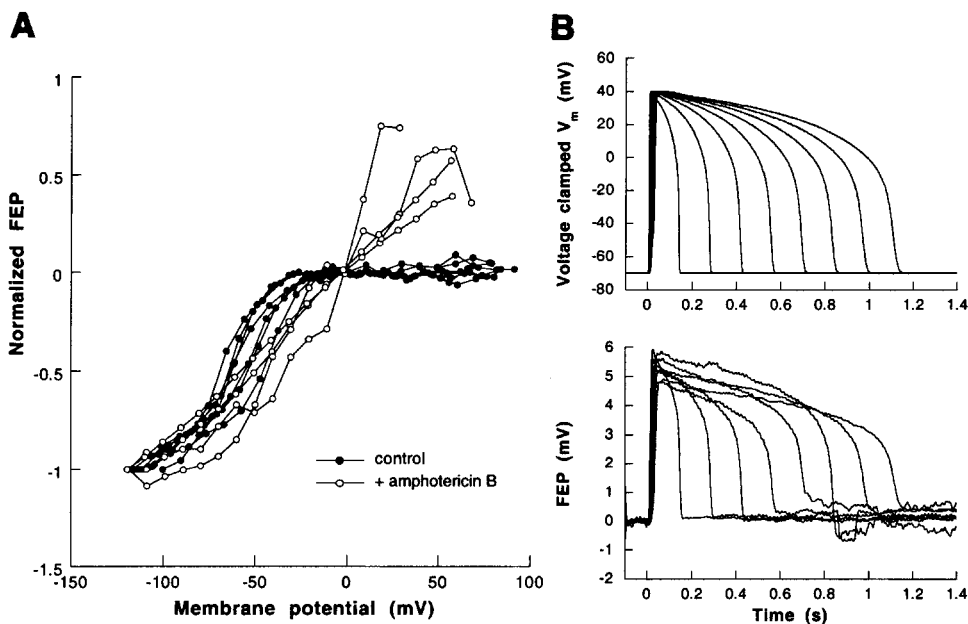
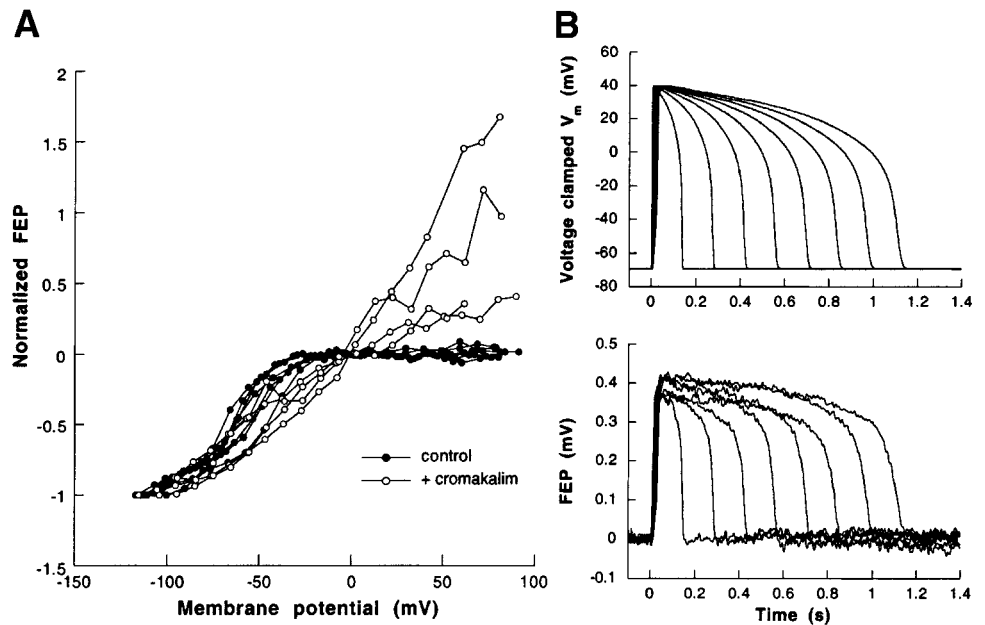


Fig. 9. FEP with 240 $\mu\text{g/ml}$ amphotericin B included in active holding pipette. *A*: normalized FEP vs. V_m for control cells without amphotericin B (closed circles, $[K^+] = 20$ or 40 mM) and with amphotericin B in the holding pipette (open circles, $[K^+] = 3$ mM). FEP was normalized by shifting each FEP-voltage relation up or down such that FEP amplitude was 0 at 0 mV, and then scaling each relation such that FEP amplitude was -1 at -120 mV. *B*: action potential clamps with amphotericin B in holding pipette. *Top*, clamped V_m . *Bottom*, FEP responses to action potential clamps.

Fig. 10. FEP with 100 $\mu\text{mol/l}$ cromakalim included in active holding pipette. *A*: normalized FEP vs. V_m for control cells without cromakalim (closed circles, $[\text{K}^+] = 20$ or 40 mM) and with cromakalim in holding pipette (open circles, $[\text{K}^+] = 40$ mM). Normalization procedure is same as for Fig. 9A. *B*: action potential clamps with cromakalim in holding pipette. *Top*, clamped V_m . *Bottom*, FEP responses to action potential clamps.



with FEPs recorded with elevated K^+ but without cromakalim (Fig. 3A).

Applications of FEP

APD/stimulus interval relation. The FEP recording technique was used to measure the relationship between stimulus interval and APD. Cells ($n = 5$) were grasped by an active pipette containing 20 mM K^+ . The reference pipette contained normal extracellular solution and was positioned freely in the bath. The cell was field stimulated at various frequencies while FEP was recorded. The durations of two successive action potentials were measured and plotted versus stimulus interval (Fig. 11A). Figure 11A shows the expected relationship in which APD decreases monotonically as stimulus interval decreases.

The FEP during cell stretch. To test the applicability of the FEP recording technique during cell stretch, the holding pipettes used to measure the FEP were also used to anchor both ends of the cell during stretch protocols. The active pipette contained 20 mM K^+ , and the reference pipette contained normal extracellular solution. Cells were mounted around the 50- μm optical fiber and field stimulated while the FEP was recorded. Periodically, during a single stimulation cycle, the cell was stretched during the action potential by displacing the optical fiber for 1,400–1,600 ms, beginning 200–500 ms before field stimulation.

Figure 11B illustrates an example of a series of FEP, length, and force recordings during 0.5-Hz field stimulation. The cell was held at its rest length during the first and third field stimuli but stretched and held at a

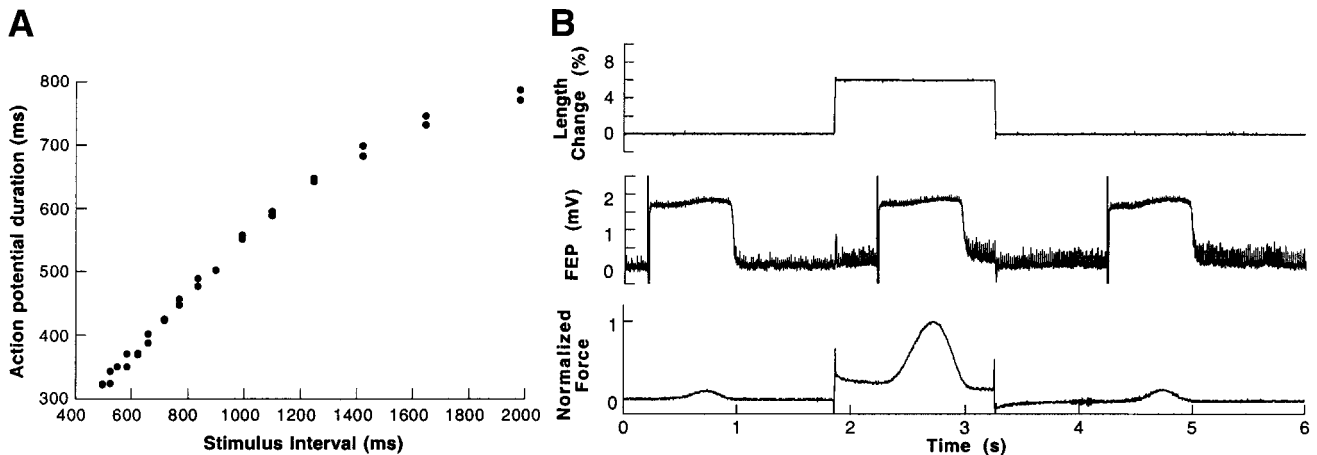


Fig. 11. Two examples of applications of FEP recording technique. *A*: stimulus frequency-duration relation measured from single cell during field stimulus pacing. Symbols mark duration of 2 successive action potentials at each pacing interval from 500–2,000 ms. *B*: length, FEP, and force recorded from one cell during pacing via 0.5-Hz field stimulation. Cell was stretched for period of 1,400 ms that encompassed one activation cycle.

6% stretch immediately before the second field stimulus. The FEP durations measured before, during, and after stretch were 761, 757, and 762 ms, respectively, indicating no significant change in APD with cell stretch. This cell was $\sim 450 \mu\text{m}$ in length.

DISCUSSION

In this study we have described a new extracellular recording technique to monitor the V_m of a cardiac myocyte. An FEP is obtained by placing a region of elevated K^+ around a cell end within a holding pipette to increase the local membrane conductance. The differential signal between the holding pipette and the bath provides a measure of the cellular V_m and is stable during mechanical perturbations of the cell. Although the FEP varies nonlinearly with V_m and is truncated in amplitude with respect to the action potential, the timing of action potential upstroke and repolarization, and therefore the APD, can be identified accurately. A linear measure of V_m cannot be obtained by varying holding pipette K^+ alone. However, the inclusion of either a voltage-insensitive pore-forming agent or an agonist for the K_{ATP} channel in the holding pipette results in an FEP that is a more linear measure of V_m and thus of action potential shape.

Origin of FEP

Figure 1A shows a simplified circuit model for a cell where the FEP is being monitored by a holding pipette during voltage or current clamp as illustrated in Fig. 1B. As the membrane properties are time and voltage dependent, it is clear that the relationship between FEP and V_m is highly nonlinear. The FEP signal can be understood as originating either from a current source set up by the depolarized membrane patch or from V_m by a voltage divider relation. In the circuit model (Fig. 1A), the current through the membrane patch is defined as $I_{m,p}$. Because the Grass P16 is a high-impedance amplifier, $I_{m,p}$ must pass entirely through the seal resistance (R_s), and therefore, $\text{FEP} = I_{m,p} R_s$. Because the FEP signal is typically much smaller than V_m , the membrane drop across the patch ($V_{m,p}$) will be approximately equal to V_m . This explains why the dependence of FEP on V_m is similar to the current-voltage relation of the membrane patch ($I_{m,p}$ vs. $V_{m,p}$, Fig. 7). Furthermore, only when $I_{m,p}$ is proportional to $V_{m,p}$ will the FEP also be proportional to V_m . The interpretation of the FEP signal as the result of a current source is analogous to that described previously for the MAP (12).

The FEP can also be thought of as originating from V_m by a voltage divider relation that involves the resistance, or reciprocal of conductance, of the membrane at the tip of the cell inside the pipette ($R_{m,p}$) and the resistance of the seal between the cell and the wall of the holding pipette (R_s , Fig. 1A), analogous to previous descriptions of the sucrose gap method (23). Because $R_{m,p}$ is voltage dependent, the magnitude of the FEP will also be voltage dependent (Fig. 7) even if R_s is constant. Factors that decrease $R_{m,p}$, such as an increased surface area of the patch or elevation of K^+ in

the holding pipette (Fig. 5), will increase the magnitude of the FEP. Similarly, an increase in R_s will also increase the FEP signal.

In principle, if a gigaohm seal could be formed, the FEP should approach the true V_m . R_s and $R_{m,p}$ can be estimated using the frog ventricular membrane model (28) implemented for the current-voltage relations in Fig. 8B. For a $[\text{K}^+]$ of 20 mM, the total ionic conductance near the resting potential is $\sim 0.05 \mu\text{S}$ for a 0.1-nF cell. Assuming a cell membrane capacitance of $1 \mu\text{F}/\text{cm}^2$, such a cell would have an area of 10^{-4}cm^2 and a conductance of $500 \mu\text{S}/\text{cm}^2$. The membrane patch inside the holding pipette is estimated to have an area of $2 \times 10^{-6} \text{cm}^2$ and therefore a conductance of $10^{-3} \mu\text{S}$, or a resistance of 1,000 M Ω . From Fig. 6, we can see that the change in the FEP signal per 20 mV change in V_m near the resting potential is on the order of 1 mV, which would correlate with an R_s of $\sim 50 \text{M}\Omega$, assuming the voltage divider configuration of Fig. 1A. Therefore, it is clear that a tight seal, but not a gigaohm seal, is formed around the cell end. Similar results were observed in all cells tested in this study. Evidently, the large size of the holding pipette tip makes a gigaohm seal impossible to form.

Figure 1A assumes that there is negligible resistance between the reference pipette electrode (attached to the V2 input of the amplifier) and the bath (ground). This is true for recordings in which the reference pipette is placed freely in the bath solution near the cell (Figs. 2–11A). However, to stretch a cell (Fig. 11B), we used the reference pipette both as a reference electrode as well as a way to grasp the free end of the cell. In this case, an additional electrical pathway analogous to the V_m -to-ground pathway through the active pipette (including R_s and $R_{m,p}$, Fig. 1A) will be created. In effect, the unipolar measurement becomes a bipolar measurement; the active pipette has an FEP-voltage relation similar to that in Fig. 7B, whereas the reference pipette has an FEP-voltage relation similar to that in Fig. 7A (because the reference pipette is filled with normal extracellular Ringer solution containing a $[\text{K}^+]$ of 3 mM). Because the resistance of the cell membrane inside the reference pipette is much higher than that of the active pipette, the active pipette potential will dominate, and the reference pipette will contribute only a small voltage signal at the V2 input to the amplifier. Alternatively, a third pipette could be added to the chamber so that the reference pipette is separate from the second holding pipette; however, we do not believe that this would improve the signal sufficiently to justify the additional technical complication.

Holding Pipette Ionic Concentrations

Potassium. The concentration of K^+ in the holding pipette must be chosen carefully. At a $[\text{K}^+]$ of 3 mM, the linear, sloped portion of the FEP-voltage relation occurs at potentials more negative than the resting potential (Fig. 7A) and therefore does not contribute to the FEP signal arising from a triggered action potential. An elevated $[\text{K}^+]$ will result in an increase in the linear range as well as the slope of the FEP-voltage relation

(Fig. 7, *B* and *C*). However, very elevated $[K^+]$ in the holding pipette will depolarize the cell. Cells not voltage-clamped were typically seen to fire spontaneous action potentials when grasped by active pipettes containing K^+ at concentrations >40 mM. This spontaneous firing started slowly and gradually increased in frequency until the cell was no longer excitable. Clearly, a balance must be achieved between obtaining a measureable and useful FEP signal and having a minimal loading or depolarizing effect on the cell.

Calcium. All presented data were recorded using an active holding pipette calcium concentration of 0.1 mM (Table 1) and a reference holding pipette calcium concentration of 1 mM. When an active holding pipette calcium concentration of 1 mM was used during initial experiments, we observed what appeared to be motion artifacts on the FEP signal caused by contraction of the tip of the cell inside the active holding pipette. This motion apparently was sufficient to change the resistance between the cell and the pipette wall, significantly impacting the FEP signal. Therefore, we used a low level of calcium (0.1 mM) in the active holding pipette for all subsequent experiments.

Other Techniques to Obtain an FEP

Because a measurable FEP signal appears only when the conductance of the cell membrane within the holding pipette increases (or the resistance of this membrane decreases), methods for further increasing local membrane conductance would be expected to create an improved FEP. Elevated K^+ increases the membrane conductance, but mainly for $V_m < 0$ mV, resulting in a nonlinear FEP-voltage relation. Augmentation of membrane conductance for $V_m > 0$ mV could linearize this relation, as was illustrated by the activation of K_{ATP} channels using cromakalim (Fig. 10). The overall FEP signal amplitude is moderately enhanced. However, because low internal ATP is also required to activate the channels, this technique would be difficult to implement in situations where there is no whole cell pipette.

Alternatively, a voltage-insensitive increase in conductance would be expected to provide a more linear relationship between V_m and the FEP. Candidates for creating a local conductance increase inside the holding pipette include an ionophore or a pore-forming antibiotic, such as nystatin, amphotericin B, or valinomycin. Results have been presented for amphotericin B, a pore-forming antibiotic nonideally selective for small cations (22) and used in the perforated patch method (25) (Fig. 9). Amphotericin B activated a large, voltage-insensitive conductance over a short time scale (<1 min), and thus the amplitude of the FEP increased significantly, a much greater increase than for trials using cromakalim. However, the cell quickly depolarized, possibly because the induced conductance was large enough to alter the normal membrane ionic gradients significantly, given that the holding pipette contained bath solution. Voltage-clamp recordings were possible ($n = 10$) for a short time (<5 min) as long as the cell was clamped to a normal resting potential. This

method of FEP recording would not be practical without a whole cell pipette to maintain the membrane potential. Valinomycin, a K^+ -selective ionophore, was also tested in some experiments ($n = 5$). Our cells did not tolerate the presence of valinomycin inside the holding pipette, so further exploration of its use was not pursued.

Therefore, even though inclusion of an agent to increase the local membrane conductance produced a larger FEP with an increased signal-to-noise ratio, this approach was found to be impractical for long-term recording. In the case of cromakalim, low internal ATP is required, which can only be assured in the presence of a whole cell pipette. Amphotericin B quickly caused the cell to depolarize unless it was voltage-clamped to a normal resting potential, also requiring a whole cell pipette. Because of these undesirable complications, solutions containing slightly elevated potassium (20–40 mM K^+) were determined to be the preferred holding pipette solutions for recording APD and cellular electrical activation in the absence of a whole cell pipette.

Comparison to Standard Patch-Clamp Techniques

The FEP is advantageous over whole cell pipette recordings under certain circumstances. Because a tight seal is not formed, exceptionally clean cell membranes and pipette tips are not required. The FEP is also readily reversible. A holding pipette can be attached and detached many times from the same cell without damage to the membrane. The FEP method has an increased mechanical stability over that of a patch pipette, because the area of contact between the cell and pipette is considerably larger. Because a direct connection is not made between the contents of the holding pipette and the intracellular solution, dialysis of the interior of the cell should be minimal. In addition, the recording of an FEP requires merely a differential amplifier and not a more expensive voltage-clamp unit.

Disadvantages of the FEP technique include the fact that the amplitude and signal-to-noise ratio of the FEP are smaller than those of V_m . Increasing the holding pipette $[K^+]$ increases the amplitude of the FEP but also produces a loading effect and depolarizes the cell. This loading effect is mitigated by the relatively small portion of membrane inside the holding pipette compared with the surface area of the remainder of the cell but nevertheless is sufficiently pronounced for $[K^+] > 40$ mM. Thus the depolarizing effect places an upper limit on the level of K^+ that is of practical use in the holding pipette. In addition, the FEP-voltage relationship is nonlinear, rectifying at positive potentials for most concentrations of pipette K^+ . Therefore, parameters such as overshoot and plateau amplitude cannot be estimated reliably.

Comparison to Related Electrophysiological Techniques

The FEP is similar to other approximations of cardiac V_m including the MAP and recordings obtained via the sucrose gap method. The MAP was first recorded in

the late 1800s by Burdon-Sanderson and Page (6) when they connected one electrode of a galvanometer to the intact surface of a frog heart and the second electrode to an injured site on the heart. Less damaging techniques, such as applying suction (10, 34) or pressure (17) at the second electrode or depolarizing the tissue using potassium chloride (8) were later found to produce similar monophasic potentials.

In the sucrose gap method for recording from cardiac tissue (14, 31), a portion of the tissue is surrounded by a pool of high K^+ solution (typically 120 mM KCl), which is electrically isolated from the normal extracellular solution bathing the rest of the preparation. This insulating barrier is formed by a nonconducting sucrose solution "gap." The high K^+ significantly depolarizes the cells in this region and creates a low resistance access to the intracellular space that allows an intracellular potential to be measured or a current to be passed for voltage clamping. Similarly, in the FEP technique, a portion of the cell is surrounded by a pool of elevated K^+ solution (20–40 mM KCl) that is electrically isolated from the normal extracellular solution bathing the rest of the cell. In this case, the insulating barrier between the solutions is formed by the wall of the tip of the glass holding pipette. Leakage current from the holding pipette to the bath solution results in only a small fraction of V_m appearing as the FEP signal.

Important characteristics differentiate the FEP signals of cells from the sucrose gap and MAP signals of tissue. First, although all of these signals are attenuated with respect to the action potential, the FEP signals are much smaller than either sucrose gap or MAP recordings. Also, the tissue-based MAP and sucrose gap procedures acquire a spatially averaged potential, whereas the FEP records exclusively from a single cell. In the cases of the MAP and sucrose gap, the cells are injured or depolarized in a defined region of tissue, and the electrical activity of surrounding cells is recorded. Unlike the case for the sucrose gap, however, the electrical "gap" in the FEP technique is not wide enough to prevent loading of the remainder of the cell by the high K^+ region. Because of this effect, the FEP technique necessarily requires a much lower $[K^+]$ than that used in the sucrose gap (20–40 mM compared with 120 mM) to reduce this loading. Consequently, just a small fraction of the cell membrane is slightly depolarized, while the rest of the cell is able to maintain its resting potential and normal electrical activity. A second major difference is that while both the MAP and sucrose gap techniques result in a monophasic signal that resembles an attenuated version of the action potential, the shape of the FEP signal is distinctly truncated in amplitude compared with V_m . Through a thorough investigation using pharmacological alterations and voltage clamps, we have shown that the FEP signal is intimately related to the current and conductance of the membrane patch inside the holding pipette, both of which are nonlinear functions of V_m that account for the truncation of the signal. In contrast, the relationship between the transmembrane potential and the MAP or sucrose gap recording is hypothesized to be

constant and nonvarying with cellular activity, so that no truncation occurs. For these reasons, the FEP technique, while similar in some respects, is not the same as the sucrose gap or the MAP methods.

FEP and Cell Stretch

The FEP recording during cellular stretch that is shown in Fig. 11*B* elucidates our motivation for developing this technique by illustrating that the FEP remains stable under conditions of cell stretch. Figure 11*B* represents one 6% stretch of nine progressively larger stretches applied to this particular cell, culminating in a final stretch of 10%. The APDs measured before, during, and after this 6% stretch were 761, 757, and 762 ms, respectively, indicating less than a 1% change in APD during stretch. However, this result by itself is not conclusive as to whether APD changes with applied stretch. Further repetitions of this experiment are required to achieve a statistically significant result.

The stretch method used in this study is designed specifically for the thin, tapered ventricular myocytes of the amphibian. This method has been used successfully to stretch frog ventricular myocytes for minutes at a time while maintaining a firm grasp on the cell ends (39). A similar stretch method utilizing double-barreled holding pipettes has been developed to attach mammalian myocytes, which have larger, blunter cell ends (24). If a sufficiently large electrical seal resistance can be achieved using this holding technique, a modified FEP recording could be feasible.

In conclusion, the FEP technique for recording electrical activity in cardiac cells is an accurate method for measuring APD and the timing of electrical activation. These quantities can be measured simply with moderately elevated levels of K^+ in the holding pipette (20 mM K^+). Because of its mechanical integrity, the FEP is a candidate to measure the electrical properties of a cell in studies of EC or ME coupling.

This work was supported by National Heart, Lung, and Blood Institute Grant R01 HL-50610. T. Riemer was a recipient of a Whitaker Foundation Graduate Fellowship in Biomedical Engineering.

Address for reprint requests and other correspondence: L. Tung, Johns Hopkins Univ., Dept. of Biomedical Engineering, 720 Rutland Ave., Traylor 703, Baltimore, MD 21205 (E-mail: ltung@bme.jhu.edu).

Received 2 July 1999; accepted in final form 18 October 1999.

REFERENCES

1. Ackerman MJ. The long QT syndrome: ion channel diseases of the heart. *Mayo Clin Proc* 73: 250–269, 1998.
2. Antzelevitch C, Shimizu W, Yan GX, and Sicouri S. Cellular basis for QT dispersion. *J Electrocardiol* 30: 168–175, 1998.
3. Billman GE. Role of ATP sensitive potassium channel in extracellular potassium accumulation and cardiac arrhythmias during myocardial ischaemia. *Cardiovasc Res* 28: 762–769, 1994.
4. Brady AJ. Mechanical properties of isolated cardiac myocytes. *Physiol Rev* 71: 413–428, 1991.
5. Bryant SM, Shipsey SJ, and Hart G. Regional differences in electrical and mechanical properties of myocytes from guinea-pig hearts with mild left ventricular hypertrophy. *Cardiovasc Res* 35: 315–323, 1997.
6. Burdon-Sanderson J and Page FJM. On the time-relations of the excitatory process in the ventricle of the heart of the frog. *J Physiol (Lond)* 2: 384–435, 1879–1880.

7. **Cheng DK-L, Tung L, and Sobie EA.** Nonuniform responses of transmembrane potential during electric field stimulation of single cardiac cells. *Am J Physiol Heart Circ Physiol* 277: H351–H362, 1999.
8. **Dower GE, Ziegler WG, Geddes MA, and Osborne JA.** Depolarizing-electrode monophasic curves and myocardial infarction ST shift. *Am J Physiol* 202: 35–40, 1962.
9. **Duceschi V, Di Micco G, Sarubbi B, Russo B, Santangelo L, and Iacono A.** Ionic mechanisms of ischemia-related ventricular arrhythmias. *Clin Cardiol* 19: 325–331, 1996.
10. **Eyster JAE, Meek WJ, Goldbert H, and Gilson WE.** Potential changes in an injured region of cardiac muscle. *Am J Physiol* 124: 717–728, 1938.
11. **Franz MR.** Mechano-electrical feedback in ventricular myocardium. *Cardiovasc Res* 32: 15–24, 1996.
12. **Franz MR.** Current status of monophasic action potential recording: theories, measurements and interpretations. *Cardiovasc Res* 41: 25–40, 1999.
13. **Garnier D.** Attachment procedures for mechanical manipulation of isolated cardiac myocytes: a challenge. *Cardiovasc Res* 28: 1758–1764, 1994.
14. **Goldman Y and Morad M.** Measurement of transmembrane potential and current in cardiac muscle: a new voltage clamp method. *J Physiol (Lond)* 268: 613–654, 1977.
15. **Hamill OP, Marty A, Neher E, Sakmann B, and Sigworth FJ.** Improved patch-clamp techniques for high-resolution current recording from cells and cell-free membrane patches. *Pflügers Arch* 391: 85–100, 1981.
16. **Han J and Moe GK.** Nonuniform recovery of excitability in ventricular muscle. *Circ Res* 14: 44–60, 1964.
17. **Jochim K, Katz LN, and Mayne W.** The monophasic electrogram obtained from the mammalian heart. *Am J Physiol* 111: 177–186, 1935.
18. **Lab MJ.** Mechanoelectric feedback (transduction) in heart: concepts and implications. *Cardiovasc Res* 32: 3–14, 1996.
19. **Lathrop DA, Contney SJ, Bosnjak ZJ, and Stowe DF.** Reversal of hypothermia-induced action potential lengthening by the K_{ATP} channel agonist bimakalim in isolated guinea pig ventricular muscle. *Gen Pharmacol* 31: 125–131, 1998.
20. **Litwin SE and Bridge JH.** Enhanced Na^+ - Ca^{2+} exchange in the infarcted heart. Implications for excitation-contraction coupling. *Circ Res* 81: 1083–1093, 1997.
21. **Maltsev VA, Sabbah HN, Tanimura M, Lesch M, Goldstein S, and Undrovinas AI.** Relationship between action potential, contraction-relaxation pattern, and intracellular Ca^{2+} transient in cardiomyocytes of dogs with chronic heart failure. *Cell Mol Life Sci* 54: 597–605, 1998.
22. **Marty A and Finkelstein A.** Pores formed in lipid bilayer membranes by nystatin: differences in its one-sided and two-sided action. *J Gen Physiol* 65: 515–526, 1975.
23. **New W and Trautwein W.** Inward membrane currents in mammalian myocardium. *Pflügers Arch* 334: 1–23, 1972.
24. **Palmer RE, Brady AJ, and Roos KP.** Mechanical measurements from isolated cardiac myocytes using a pipette attachment system. *Am J Physiol Cell Physiol* 270: C697–C704, 1996.
25. **Rae J, Cooper K, Gates P, and Watsky M.** Low access resistance perforated patch recordings using amphotericin B. *J Neurosci Methods* 37: 15–26, 1991.
26. **Ravens U, Wettwer E, Pfeifer T, Himmel H, and Armah B.** Characterization of the effects of the new inotropic agent BDF 9148 in isolated papillary muscles and myocytes of the guinea-pig heart. *Br J Pharmacol* 104: 1019–1023, 1991.
27. **Riemer TL, Fan J-S, and Tung L.** Are swelling, pressure, and axial stretch equivalent stimuli for mechano-electrical coupling in heart cells? (Abstract). *International Workshop: Mechano-Electrical Feedback and Cardiac Arrhythmias*, Trento, Italy, 1997, p. 28.
28. **Riemer TL, Sobie EA, and Tung L.** Stretch-induced changes in arrhythmogenesis and excitability in experimentally based heart cell models. *Am J Physiol Heart Circ Physiol* 275: H431–H442, 1998.
29. **Riemer TL and Tung L.** A novel extracellular method to measure cardiac action potential duration during cell stretch (Abstract). *Ann Biomed Eng* 26, Suppl: S-19, 1998.
30. **Riemer TL and Tung L.** Basis of a focal extracellular potential measured from cardiac myocytes (Abstract). *Biophys J* 76: A267, 1999.
31. **Rougier O, Vassort G, and Stämpfli R.** Voltage clamp experiments of frog atrial heart muscle fibres with the sucrose gap technique. *Pflügers Arch* 301: 91–108, 1968.
32. **Sasaki N, Mitsuiye T, and Noma A.** Effects of mechanical stretch on membrane currents of single ventricular myocytes of guinea-pig heart. *Jpn J Physiol* 42: 957–970, 1992.
33. **Schaffer P, Ahammer H, Muller W, Koidl B, and Windisch H.** Di-4-ANEPPS causes photodynamic damage to isolated cardiomyocytes. *Pflügers Arch* 426: 548–551, 1994.
34. **Schütz E.** Weitere Versuche mit einphasischer Aufzeichnung des Warmblüter-Elektrokardiogramms. *Z Biol* 95: 77–90, 1934.
35. **Shepherd N, Vornanen M, and Isenberg G.** Force measurements from voltage-clamped guinea pig ventricular myocytes. *Am J Physiol Heart Circ Physiol* 258: H452–H459, 1990.
36. **Shigematsu S, Kiyosue T, Sato T, and Arita M.** Rate-dependent prolongation of action potential duration in isolated rat ventricular myocytes. *Basic Res Cardiol* 92: 123–128, 1997.
37. **Tarr M, Trank JW, and Goertz KK.** Voltage-tension relations in single frog atrial cardiac cells. *Circ Res* 59: 447–455, 1986.
38. **Tung L, Sliz N, and Mulligan MR.** Influence of electrical axis of stimulation on excitation of cardiac muscle cells. *Circ Res* 69: 722–730, 1991.
39. **Tung L and Zou S.** Influence of stretch on excitation threshold of single frog ventricular cells. *Exp Physiol* 80: 221–235, 1995.
40. **Vornanen M, Shepherd N, and Isenberg G.** Tension-voltage relations of single myocytes reflect Ca release triggered by Na/Ca exchange at 35°C but not 23°C. *Am J Physiol Cell Physiol* 267: C623–C632, 1994.
41. **White E, Le Guennec JY, Nigretto JM, Gannier F, Argibay JA, and Garnier D.** The effects of increasing cell length on auxotonic contractions; membrane potential and intracellular calcium transients in single guinea-pig ventricular myocytes. *Exp Physiol* 78: 65–78, 1993.
42. **Yan GX, Shimizu W, and Antzelevitch C.** Characteristics and distribution of M cells in arterially perfused canine left ventricular wedge preparations. *Circulation* 98: 1921–1927, 1998.